Detection of Tethered Biocide Moiety Segregation to Silicone Surface Using Sum Frequency Generation Vibrational Spectroscopy

Shuji Ye,[†] Arthur McClelland,[‡] Partha Majumdar,[§] Shane J. Stafslien,[§] Justin Daniels,[§] Bret Chisholm,[§,||] and Zhan Chen*[,†,‡]

Department of Chemistry and Applied Physics Program, University of Michigan, Ann Arbor, Michigan 48109, and Center for Nanoscale Science and Engineering and Department of Coatings and Polymeric Materials, North Dakota State University, Fargo, North Dakota 58102

Received March 11, 2008. Revised Manuscript Received April 14, 2008

Polymer surface properties are controlled by the molecular surface structures. Sum frequency generation (SFG) vibrational spectroscopy has been demonstrated to be a powerful technique to study polymer surface structures at the molecular level in different chemical environments. In this research, SFG has been used to study the surface segregation of biocide moieties derived from triclosan (TCS) and tetradecyldimethyl (3-trimethoxysilylpropyl) ammonium chloride (C-14 QAS) that have been covalently bound to a poly(dimethylsiloxane) (PDMS) matrix. PDMS materials are being developed as coatings to control biofouling. This SFG study indicated that TCS-moieties segregate to the surface when the bulk concentration of TCS-moieties exceeds 8.75% by weight. Surface segregation of C-14 QAS moieties was detected after 5% by weight incorporation into a PDMS matrix. SFG results were found to correlate well with antifouling activity, providing a molecular interpretation of such results. This research showed that SFG can aid in the development of coatings for controlling biofouling by elucidating the chemical structure of the coating surface.

1. Introduction

Polymer materials are used extensively in aqueous environments. Examples include biomedical polymer implants and marine antibiofouling polymer coatings. In both cases, the performance of polymer materials is determined by their surface properties. The surface properties are mediated by molecular surface structures. Many surface-sensitive analytical techniques require high vacuum to operate; therefore, they cannot provide molecular structural information of polymer surfaces in an aqueous environment. This study used a nonlinear optical laser spectroscopy technique, sum frequency generation (SFG) vibrational spectroscopy, to investigate the molecular-level surface structures of polymers for antibiofouling applications. The understanding of molecular surface structures of polymer materials in an aqueous environment will facilitate the design of polymer surfaces with improved antibiofouling performance.

Biofouling, the growth of marine organisms on the hulls of ocean-going vessels, causes many problems such as extra financial burdens and excessive consumption of energy.[1] Minimally adhesive polymers or polymers from which foulants can be easily removed (e.g., polydimethylsiloxane (PDMS)), are being developed as coatings for use in the marine environment.[2−15] The physical nature of PDMS materials enables PDMS coatings to retard the onset of fouling and provide easy release when fouling does occur. It is generally believed that the good fouling-release performance of PDMS coatings is due to their low surface energy,[9,10] low glass transition temperature,[11] and low elastic modulus.[12,13]

The possibility to use materials with nonleaching, chemically bound biocide moieties for the control of marine biofouling has also been explored recently.[15,16] Traditional antifouling coatings are based on leachable biocides that cause a negative environmental impact. The authors investigated hybrid coatings that possess characteristics of both fouling-release and antifouling coatings by tethering biocides to PDMS matrices.[16−18] In order to design such surfaces, it is necessary to ensure that both PDMS and biocide moieties are present on the coating surface. Therefore, it is crucial to characterize molecular chemical structures of coating surfaces. Since such materials will be used in the aqueous environment, it is also essential to study the surface structures *in situ*. As mentioned above, many high-vacuum surface analytical techniques cannot be applied to study surfaces in an aqueous

* To whom all correspondence should be addressed. Email: zhanc@umich.edu. Fax: 734-647-4865.

[†] Department of Chemistry, University of Michigan.

[‡] Applied Physics Program, University of Michigan.

[§] Center for Nanoscale Science, North Dakota State University.

[||] Department of Coatings and Polymeric Materials, North Dakota State University.

(1) Rittschof, D. In *Marine Chemical Ecology*; McClintock, J. B., Baker, B. J., Eds.; CRC Press: Boca Raton, 2001; pp 543−566.

(2) Hogt, A. H.; Gregonis, D. E.; Andrade, J. D.; Kim, S. W.; Dankert, J.; Feijen, J. *J. Colloid Interface Sci.* **1985**, *106*, 289–298.

(3) Holmstrom, C.; Kjelleberg, S. *Biofouling* **1994**, *8*, 147–160.

(4) Adkins, J. D.; Mera, A. E.; Roeshort, M. A.; Pawlikowski, G. T.; Brady, R. F. *Prog. Org. Coat.* **1996**, *29*, 1–5.

(5) Petronis, S.; Berntsson, K.; Gold, J.; Gatenholm, P. *J. Biomater. Sci., Polym. Ed.* **2000**, *11*, 1051–1072.

(6) Morra, M. *J. Biomater. Sci., Polym. Ed.* **2000**, *11*, 547–569.

(7) Berglin, M.; Larsson, A.; Jonsson, P. R.; Gatenholm, P. *J. Adhes. Sci. Technol.* **2001**, *15*, 1485–1502.

(8) Callow, M. E.; Jennings, A. R.; Brennan, A. B.; Seegert, C. E.; Gibson, A.; Wilson, L.; Feinberg, A.; Baney, R.; Callow, J. A. *Biofouling* **2002**, *18*, 237–245.

(9) Baier, R. E. In *Proceedings of the 3rd International Congress on Marine Corrosion and Fouling*; Acker, R. F., Brown, B. R., DePalma. J. R., Iverson, W. P., Eds.; Northwestern University Press: Evanston, IL, 1973; pp 633−639.

(10) Dexter, S. C.; Sullivan, J. D.; Iii, J. W.; Watson, S. W. *Appl. Microbiol.* **1975**, *30*, 298–308.

(11) Mera, A. E.; Fox, R. B.; Bullock, S.; Wynne, K. J. In *Proceedings of the 21st Annual Meeting of the Adhesion Society*; Savannah, GA, 1998; pp 138−140.

(12) Brady, R. F., Jr.; Singer, I. L. *Biofouling* **2000**, *15*, 73–81.

(13) Sun, Y.; Guo, S.; Walker, G. C.; Kavanagh, C. J.; Swain, G. W. *Biofouling* **2004**, *20*, 279–289.

(14) Barrios, C. A.; Xu, Q. W.; Cutright, T.; Newby, B. Z. *Colloid Surf., B* **2005**, *41*, 83–93.

(15) Thomas, J.; Choi, S. B.; Fjeldheim, R.; Boudjouk, P. *Biofouling* **2004**, *20*, 227–236.

(16) Majumdar, P.; Lee, E.; Ward, K.; Chisholm, B. *Polym. Prepr. (Am. Chem. Soc., Div. Polym. Chem.)* **2007**, *48*, 165–166.

(17) Choi, S. B.; Jepperson, J.; Thomas, J.; Jarabek, L.; Chisholm, B.; Boudjouk, F. *IUPAC-PSK30* **2006**, 378.

(18) Stafslien, S. J.; Daniels, J.; Chisholm, B. J.; Christianson, D. A. *Biofouling* **2007**, *23*, 37–44.

10.1021/la800769z CCC: $40.75 © 2008 American Chemical Society
Published on Web 07/31/2008

environment. Among the surface techniques that do not require high vacuum,[19–25] one of the most widely used methods to study surfaces of wet polymer materials is measurement of water contact angle. Dynamic contact angle (DCA) experiments can be used to qualitatively evaluate the heterogeneity or structure reorganization of polymer surfaces, but no detailed chemical information can be deduced from such studies.[19–21,25] Freeze−drying X-ray photoelectron spectroscopy (XPS) can detect the surface composition change of the polymer upon contacting water, but the sample handling tends to be complicated and no orientation information about surface chemical groups can be obtained.[22] AFM has also been applied to follow surface reorganizations in water,[23,24] but in most cases, only surface morphological changes, rather than molecular chemical structural changes, can be observed.

Sum frequency generation (SFG) vibrational spectroscopy has previously been applied to the study of polymer surface restructuring in water.[26–28] SFG can provide information such as functional group composition and orientation at a surface or interface with a submonolayer sensitivity.[29–35] In addition, SFG can be used to study *in situ* surface restructuring behavior of polymer materials in water.[36] SFG studies have indicated that different polymer surfaces exhibit markedly different surface restructuring behaviors in water. Some polymers show no surface changes in water,[28] while other polymer surfaces can have immediate and reversible side chain orientation changes,[28] immediate and irreversible backbone changes,[37–39] or slow changes in water.[26]

SFG studies on several model PDMS materials have been previously reported.[36] Molecular surface structures of these PDMS materials in air, in water, and in a hydrophobic fluorinated solvent have been studied.[36] In this paper, SFG has been used to characterize the surface structures of PDMS coatings containing different levels of tethered biocide moieties in air and in water. The two biocides used to generate the PDMS coatings investigated were 5-chloro-2-(2,4-dichlorophenoxy)phenol (triclosan or TCS) and tetradecyldimethyl(3-trimethoxysilylpropyl)ammonium chloride (C-14 QAS). SFG has also been used to study molecular interactions between the well-studied protein, fibrinogen, and the PDMS coating with TCS incorporated. The antifouling performance of the PDMS materials containing tethered biocide moieties was determined using two different marine microorganisms: a marine bacterium, *Cellulophaga lytica*, and an algal species, *Navicula incerta*. The results from SFG studies were correlated to antifouling performance to provide a molecular-level understanding of the antifouling results.

Table 1. Description of the PDMS-TCS Samples Prepared

sample ID	wt fraction HMS-TCS to T-2 translucent base	wt % TCS-moieties
A0	0[a]	0
A1	10/90	5
A2	17.5/82.5	8.75
A3	25/75	12.5
A4	37.5/62.5	18.75
A5	50/50	25

[a] Made with 7 wt % Silastic T-2 curing agent.

2. Experimental Section

2.1. Materials. Silastic T-2 Translucent Base (a mixture of PDMS and organically modified silica) and Silastic T-2 Curing Agent were purchased from Dow Corning Corporation. Silanol-terminated PDMS with a molecular weight of 18 000 (DMS-S27), methyltriacetoxysilane (SIM6519.0), tetradecyldimethyl (3-trimethoxysilylpropyl)-ammonium chloride (C-14 QAS) as a 50 wt % solution in methanol, and 50−55% methylhydrosiloxane-dimethylsiloxane copolymer (HMS-501) were purchased from Gelest, Inc. (Tullytown, PA,USA). 1.0 M tetrabutylammonium fluoride (TBAF) in tetrahydrofuran, platinum oxide, 4-methyl-2-pentanone (MIBK), and 5-chloro-2-(2-,4-dichlorophenoxy)phenol (TCS) were purchased from Aldrich (Milwaukee, WI, USA). Biofilm growth medium (BGM) consisted of 0.5 g of peptone and 0.1 g of yeast extract per liter of deionized water and was sterilized with a 0.2 μm vacuum cap membrane filter.

2.1.1. Synthesis of a Hydride-Functional PDMS Containing TCS Moieties (HMS-TCS). 50 g of allyl triclosan, synthesized as previously described by Thomas and co-workers,[15] and 50 g of HMS-501 were dissolved in 289 g of toluene, and the mixture was heated to 90 °C. Next, 100 mg of platinum oxide was added and the mixture was held at 90 °C for 24 h. Progress of the hydrosilylation reaction was monitored using proton nuclear magnetic resonance spectroscopy by observing the conversion of protons associated with the vinyl group of allyl triclosan group to methylene protons. Upon completion of the reaction, platinum oxide was removed by passing the reaction mixture through a column packed with neutral alumina. The polymer was isolated by vacuum stripping of the toluene using a rotary evaporator.

2.1.2. Preparation of Coatings Containing Tethered TCS Moieties. Coatings containing tethered TCS moieties were prepared by replacing the curing agent used with the commercially available, addition-cured PDMS sold by Dow Corning under the trade name Silastic T-2, with HMS-TCS. The preparation procedure is as follows: Silastic T-2 translucent base was dissolved 50% by weight in MIBK. Six samples of PDMS-TCS possessing different levels of tethered TCS moieties were made by adding various concentrations of HMS-TCS to the T-2 base solution and mixing thoroughly. The details of the composition of the six coating samples are shown in Table 1. Specimens for SFG studies were made by spin-coating samples onto fused silica substrates or CaF_2 prisms immediately after thoroughly mixing the T-2 base solution and the curing agents. The samples were then cured for 24 h at room temperature. A general molecular formula of PDMS incorporated with biocides and the formula for the curing agent incorporated with TCS are shown in Figure 1.

(19) Uilk, J. M.; Mera, A. E.; Fox, R. B.; Wynne, K. J. *Macromolecules* **2002**, *36*, 3689–3694.
(20) Bertolucci, M.; Galli, G.; Chiellini, E.; Wynne, K. J. *Macromolecules* **2004**, *37*, 3666–3672.
(21) Mera, A. E.; Goodwin, M.; Pike, J. K.; Wynne, K. J. *Polymer* **1999**, *40*, 419–427.
(22) Hawkridge, A. M.; Gardella, J. A.; Toselli, M. *Macromolecules* **2002**, *35*, 6533–6538.
(23) Gudipati, C. S.; Johnson, J. A.; Wooley, K. L. *Polym. Prepr. (Am. Chem. Soc., Div. Polym. Chem.)* **2004**, *45*, 105.
(24) LeMieux, M. C.; Peleshanko, S.; Anderson, K. D.; Tsukruk, V. V. *Langmuir* **2007**, *23*, 265–273.
(25) Pike, J. K.; Ho, T.; Wynne, K. J. *Chem. Mater.* **1996**, *8*, 856–860.
(26) Zhang, D.; Ward, R. S.; Shen, Y. R.; Somorjai, G. A. *J. Phys. Chem. B* **1997**, *101*, 9060–9064.
(27) Chen, C. Y.; Even, M. A.; Wang, J.; Chen, Z. *Macromolecules* **2002**, *35*, 9130–9135.
(28) Wang, J.; Woodcock, S. E.; Buck, S. M.; Chen, C. Y.; Chen, Z. *J. Am. Chem. Soc.* **2001**, *123*, 9470–9471.
(29) Ye, S.; Noda, H.; Morita, S.; Uosaki, K.; Osawa, M. *Langmuir* **2003**, *19*, 2238–2242.
(30) Chen, C.; Wang, J.; Woodcock, S. E.; Chen, Z. *Langmuir* **2002**, *18*, 1302–1309.
(31) Oh-E, M.; Lvovsky, A. I.; Wei, X.; Shen, Y. R. *J. Chem. Phys.* **2000**, *113*, 8827–8832.
(32) Zhuang, X.; Miranda, P. B.; Kim, D.; Shen, Y. R. *Phys. Rev. B* **1999**, *59*, 12632–12640.
(33) Miranda, P. B.; Shen, Y. R. *J. Phys. Chem. B* **1999**, *103*, 3292–3307.
(34) Miranda, P. B.; Pflumio, V.; Saijo, H.; Shen, Y. R. *Chem. Phys. Lett.* **1997**, *264*, 387–392.
(35) Chen, Z. *Polym. Int.* **2007**, *56*, 577–587.
(36) Chen, C. Y.; Wang, J.; Chen, Z. *Langmuir* **2004**, *20*, 10186–10193.
(37) Chen, Q.; Zhang, D.; Somorjai, G. A.; Bertozzi, C. R. *J. Am. Chem. Soc.* **1999**, *121*, 446–447.
(38) Dreesen, L.; Humbert, C.; Hollander, P.; Mani, A. A.; Ataka, K. *Chem. Phys. Lett.* **2001**, *333*, 327–331.
(39) Chen, C. Y.; Clarke, M. L.; Wang, J.; Chen, Z. *Phys. Chem. Chem. Phys.* **2005**, *7*, 2357–2363.
(40) Perry, A.; Neipert, C.; Space, B.; Moore, P. B. *Chem. Rev.* **2006**, *106*, 1234–1258.

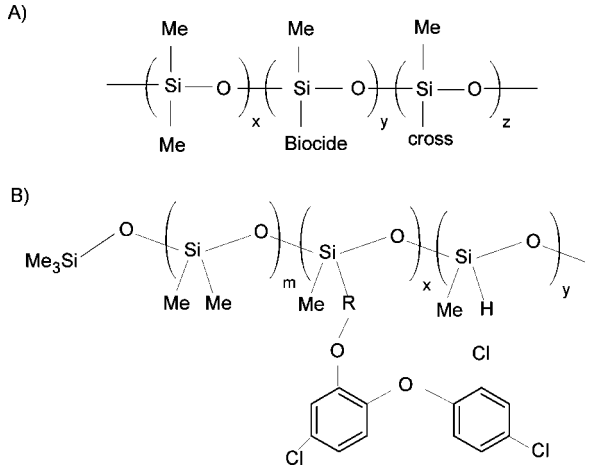

Figure 1. (A) Molecular formula of PDMS incorporated with biocide. (B) Curing agent with TCS incorporated.

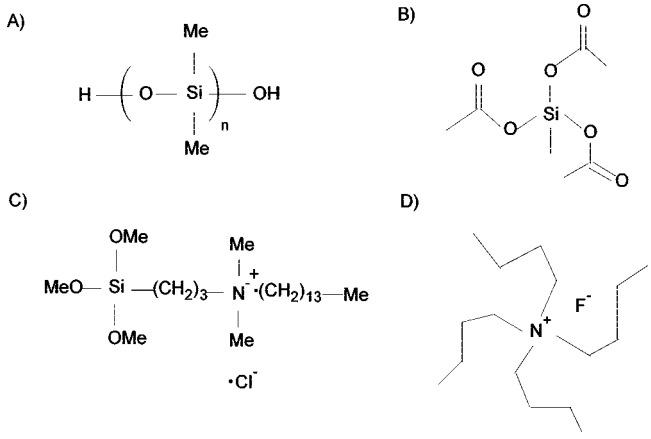

Figure 2. Molecular formulas of the materials used to prepare PDMS incorporated with C-14 QAS. (A) Silanol-terminated polydimethylsiloxane. (B) Cross-linker, methyltriacetoxysilane. (C) C-14 QAS. (D) Catalyst, tetrabutylammonium fluoride.

2.1.3. Preparation of Coatings Containing Tethered C-14 QAS Moieties. Molecular formulas of the materials used to prepare PDMS incorporated with C-14 QAS including silanol-terminated PDMS cross-linker (methyltriacetoxysilane), C-14 QAS, and catalyst (tetrabutylammonium fluoride) are shown in Figure 2. 50 mM TBAF catalyst solution was prepared by dispensing 1.25 mL of 1.0 M TBAF solution in a 25 mL volumetric flask and adding MIBK volumetrically up to 25 mL. Coating samples were prepared by solution blending 700 mg DMS-S27, 105 mg methyltriacetoxysilane, 105 mg TBAF solution, and C-14 QAS in the amount described in Table 2. The coating solutions were continually stirred overnight and then spin-coated on fused silica windows and stored under ambient conditions for 24 h. The specimens were then cured overnight at 50 °C.

2.2. SFG. Details about SFG theory have been reported previously.[40–46] In a typical SFG experiment, two pulsed laser beams, one with a fixed frequency in the visible frequency range (ω_{Vis}), and one with a tunable frequency in the infrared frequency range (ω_{IR}), are overlapped spatially and temporally on the sample. A third beam, the SFG signal, is generated at the sum frequency of the two input beams by the nonlinear process, $\omega_{SF} = \omega_{Vis} + \omega_{IR}$. The intensity of the light at ω_{SF} is proportional to the square of the sample's second-order nonlinear susceptibility $\chi_{eff}^{(2)}$ (see eq 1), which vanishes when a material has inversion symmetry.

$$I(\omega) \propto |\chi_{eff}^{(2)}|^2 I_1(\omega_1) I_2(\omega_2) \quad (1)$$

Therefore, bulk materials that possess inversion symmetry do not generate a sum frequency signal, but surfaces where the symmetry is broken do generate a sum frequency signal. As the IR beam frequency is tuned over the vibrational resonance of surface/interface molecules, the effective surface nonlinear optical susceptibility $\chi_{eff}^{(2)}$ can be enhanced. The frequency dependence of $\chi_{eff}^{(2)}$ is described by

$$\chi_{eff}^{(2)}(\omega) = \chi_{NR}^{(2)} + \sum_q \frac{A_q}{\omega - \omega_q + i\Gamma_q} \quad (2)$$

where A_q, ω_q, and Γ_q are the strength, resonant frequency, and damping coefficient of the vibrational mode q respectively, and $\chi_{NR}^{(2)}$ is the nonresonant background.[46–51] The plot of SFG signal vs the IR input frequency shows a polarized vibrational spectrum of the surface or interface.

Both theoretical calculations and experimental results show that SFG is submonolayer sensitive.[43–60] The authors' SFG system has been described in detail previously.[27,47,52,53] In this research, SFG spectra with different polarization combinations including ssp (s-polarized SF output, s-polarized visible input, and p-polarized infrared input) and ppp were collected with two input laser beams traveling through the fused silica windows or CaF_2 prisms and overlapping on the polymer/air, polymer/water, or polymer/protein solution interface. All SFG spectra were normalized by the intensities of the input IR and visible beams. The authors' previous research has demonstrated that SFG signals are dominated by the polymer/air or polymer/liquid interface, with almost no polymer/substrate or polymer bulk contributions to the spectra using this experimental geometry.[27,47,52,53]

2.3. FTIR Experiments. FTIR spectra were obtained using a Nicolet Magna-IR 550 spectrometer. Spectra collected were averages of 256 scans at a 2 cm^{-1} resolution.

2.4. Measurement of Antifouling Activity. The method for measuring leachate toxicity has been reported previously.[61] Preconditioned coatings were incubated in 1.0 mL of growth medium overnight (~18 h) and the resultant coating leachates were collected. 0.05 mL of a *C. lytica* suspension in BGM (~10^7 cells/mL) or of

(41) Buck, M.; Himmelhaus, M. *J. Vac. Sci. Technol. A* **2001**, *19*, 2717–2736.
(42) Chen, Z.; Shen, Y. R.; Somorjai, G. A. *Annu. Rev. Phys. Chem.* **2002**, *53*, 437–465.
(43) Shen, Y. R. *The Principles of Nonlinear Optics*; John Wiley & Sons: New York, 1984.
(44) Chen, Z.; Gracias, D. H.; Somorjai, G. A. *Appl. Phys. B: Laser Opt.* **1999**, *68*, 549–557.
(45) Shen, Y. R. *Appl. Phys. A: Mater. Sci. Process* **1994**, *59*, 541–543.
(46) Hirose, C.; Akamatsu, N.; Domen, K. *Appl. Spectrosc.* **1992**, *46*, 1051–1072.
(47) Wang, J.; Chen, C. Y.; Buck, S. M.; Chen, Z. *J. Phys. Chem. B* **2001**, *105*, 12118–12125.
(48) Gautam, K. S.; Dhinojwala, A. *Macromolecules* **2001**, *34*, 1137–1139.
(49) Hirose, C.; Yamamoto, H.; Akamatsu, N.; Domen, K. *J. Phys. Chem.* **1993**, *97*, 10064–10069.
(50) Hirose, C.; Akamatsu, N.; Domen, K. *J. Chem. Phys.* **1992**, *96*, 997–1004.
(51) Kim, J.; Somorjai, G. A. *J. Am. Chem. Soc.* **2003**, *125*, 3150–3158.
(52) Chen, C. Y.; Wang, J.; Even, M. A.; Chen, Z. *Macromolecules* **2002**, *35*, 8093–8097.
(53) Wang, J.; Paszti, Z.; Even, M. A.; Chen, Z. *J. Am. Chem. Soc.* **2002**, *124*, 7016–7023.
(54) Gautam, K. S.; Schwab, A. D.; Dhinojwala, A.; Zhang, D.; Dougal, S. M.; Yeganeh, M. S. *Phys. Rev. Lett.* **2000**, *85*, 3854–3857.
(55) Opdahl, A.; Somorjai, G. A. *Langmuir* **2002**, *18*, 9409–9412.
(56) Zhang, D.; Dougal, S. M.; Yeganeh, M. S. *Langmuir* **2000**, *16*, 4528–4532.
(57) Chen, C. Y.; Even, M. A.; Chen, Z. *Macromolecules* **2003**, *36*, 4478–4484.
(58) Chen, C. Y.; Loch, C. L.; Wang, J.; Chen, Z. *J. Phys. Chem. B* **2003**, *107*, 10440–10445.
(59) Wang, J.; Even, M. A.; Chen, X. Y.; Schmaier, A. H.; Waite, J. H.; Chen, Z. *J. Am. Chem. Soc.* **2003**, *125*, 9914–9915.
(60) Chen, C. Y.; Wang, J.; Loch, C. L.; Chen, Z. *J. Am. Chem. Soc.* **2004**, *126*, 1174–1179.
(61) Majumdar, P.; Lee, E.; Patel, N.; Ward, K.; Stafslien, S. J.; Daniels, J.; Chisholm, B.; Boudjouk, P.; Callow, M. E.; Callow, J. A.; Thompson, S. E. M. *Biofouling* **2008**, *24*, 185–200.

Table 2. Formulations Based on Silanol PDMS(DMS-S27) and C-14 QAS

sample	DMS-S27 (mg)	cross-linker (methyltriacetoxysilane) (mg)	catalyst solution (50 mM TBAF) (mg)	C-14 QAS (mg)	C-14 QAS (M/100 mg PDMS)
B0	700	105	105	0	0
B1	700	105	105	31	0.01
B2	700	105	105	62	0.02
B3	700	105	105	92	0.03
B4	700	105	105	123	0.04
B5	700	105	105	154	0.05
B6	700	105	105	185	0.06

a *N. incerta* suspension in Guillard's F/2 medium ($\sim 10^5$ cells/mL) was added to 1.0 mL of each coating leachate. 0.2 mL of each coating leachate, with the addition of *C. lytica* or *N. incerta*, was transferred in triplicate to a 96-well polystyrene plate. *C. lytica* plates were incubated for 18 h at 28 °C, while *N. incerta* plates were incubated for 48 h at 18 °C in an illuminated growth cabinet with a 16:8 light/dark cycle (photon flux density 330 μmol photon/m^2 s). *C. lytica* plates were rinsed three times with deionized water and stained with 0.5 mL of crystal violet. 0.5 mL of glacial acetic acid was added to each well to extract the crystal violet dye, and absorbance measurements were made at 600 nm with a multiwell plate reader. *N. incerta* plates were measured for fluorescence of chlorophyll (excitation 360 nm; emission 670 nm). A significant reduction in the amount of biofilm growth obtained relative to PDMS leachate was considered to be a consequence of toxic components leaching into the overlying medium.

The rapid evaluation of bacterial biofilm growth and retention on coatings cast in multiwell plates has been reported previously.[18,62,63] Briefly, coating plates were inoculated with a 1.0 mL suspension of *C. lytica* in BGM ($\sim 10^7$ cells/mL). The plates were then incubated statically in a 28 °C incubator for 18 h to facilitate bacterial attachment and subsequent colonization. The plates were then rinsed three times with 1.0 mL of deionized water to remove any planktonic or loosely attached biofilm. The biofilm retained on each coating surface after rinsing was then stained with crystal violet. Digital images were taken of each coating array plate, and percent surface coverage measurements were made for each coating using an automated software tool.[64] Next, the crystal violet dye was extracted from the biofilm with addition of 0.5 mL of glacial acetic acid and the resulting eluate was measured for absorbance at 600 nm. The absorbance values obtained were directly proportional to the amount of biofilm retained on the coating surface. Each data point was reported as the mean absorbance or percent coverage value of three replicate wells. Error bars represent 1 standard deviation of the absorbance ratio.

The rapid evaluation of algal biofilm growth on coatings cast in multiwell plates has been reported previously.[65] Briefly, a 1.0 mL suspension of *N. incerta* in F/2 medium ($\sim 10^5$ cells/mL) was delivered to each coating plate. Plates were incubated statically for 48 h at the same conditions detailed for leachate toxicity evaluations. Biomass was quantified by the fluorescence of chlorophyll, which was extracted from biomass in the well with 1.0 mL of DMSO. The plates were incubated in darkness for 30 min, and 0.2 mL of the resulting eluate was pipetted from each well into wells of a 96 well plate and the fluorescence was measured (excitation wavelength 360 nm; emission wavelength 670 nm). Fluorescence was recorded as relative fluorescence units (RFU). Each data point was reported as the mean RFU value of three replicate wells. Error bars represent 1 standard deviation of the RFU ratio.

3. Results and Discussion

3.1. Surface Structures of PDMS with TCS Incorporated.

3.1.1. Surface Structures in Air. Figure 3 shows SFG spectra collected from PDMS-TCS coatings using the ssp polarization combination. All SFG spectra presented in Figure 3 are dominated by the peaks contributed by the C−H symmetric and asymmetric stretches of the Si-CH_3 group at 2910 and 2965 cm^{-1}. Because TCS only contains aromatic C−H groups, its C−H stretching peaks should appear at higher than 3000 cm^{-1}, but no such signal was detected in our experiments. This may indicate that, in air, the surfaces of the samples are completely covered by PDMS and the TCS moieties do not segregate to these surfaces. This is reasonable because PDMS has a very low surface energy in air.

3.1.2. Surface Structures in Water. Since the PDMS-TCS coatings are being investigated for potential application as marine coatings, it is their surface composition in water rather than that in air will determine their performance. SFG spectra were collected from surfaces of samples while in contact with water (Figure 4). Compared to spectra collected in air, only very weak or no SFG signals between 2900 and 2965 cm^{-1} were detected from the surfaces of samples when in contact with water. The significant decrease in SFG signal intensity of the peaks at 2910 cm^{-1} and 2965 cm^{-1} may be due to several factors such as the following: The Fresnel coefficients of the polymer/air and polymer/water interfaces are different;[27,28,53] the polymer surface in water may be more disordered; the $SiCH_3$ groups on the surface can have different orientations in air and in water; or the TCS moieties segregate to the surface more in water. Since the TCS moieties are more hydrophilic than PDMS, they may segregate to the coating surface in water. However, no aromatic C−H stretching signals were observed from any of the coating surfaces when in contact with water. The absence of the aromatic signals may be due to the weakness of such signals.

An SFG process is a combination of an infrared absorption process and an anti-Stokes Raman scattering process. The SFG hyperpolarizability of a vibrational mode is a product of the IR transition dipole moment and the Raman polarizability. Therefore,

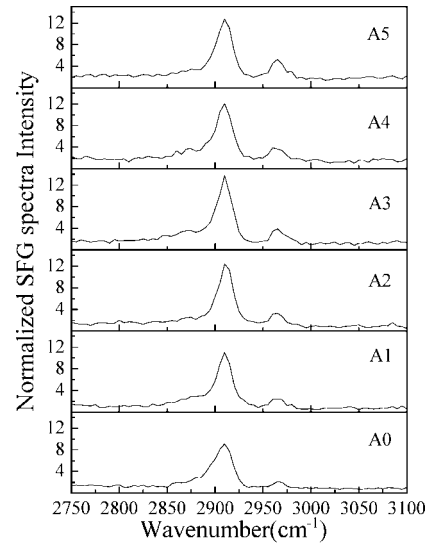

Figure 3. SFG spectra (ssp) collected from PDMS samples with different amounts of TCS incorporated in air.

(62) Stafslien, S. J.; Bahr, J. A.; Feser, J. M.; Weisz, J. C.; Chisholm, B. J.; Ready, T. E.; Boudjouk, P. *J. Comb. Chem* **2006**, *8*, 156–162.

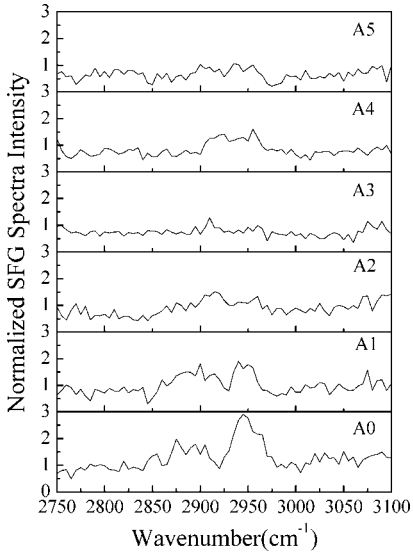

Figure 4. SFG (ssp) spectra collected from PDMS samples with different amounts of TCS incorporated in water.

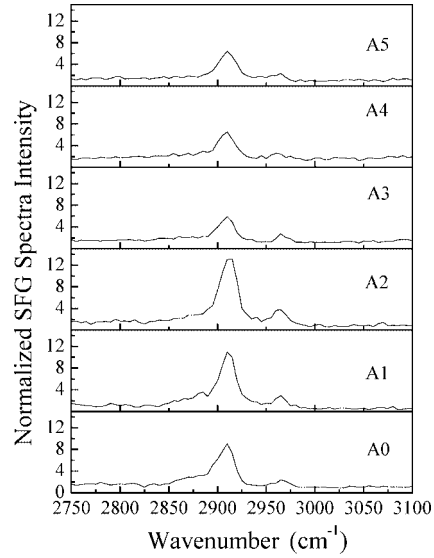

Figure 5. SFG (ssp) spectra collected from the samples with different amounts of TCS incorporated after contact with water and exposure to air again.

a strong SFG signal of a vibrational mode requires that the IR signal of the same mode cannot be too weak. FTIR transmission spectra of various coating samples listed in Table 1 were collected (see Supporting Information). These spectra indicate that the FTIR absorbance is very small for aromatic C−H stretches at 3065 cm^{-1} from TCS groups for all six coatings. An FTIR spectrum of HMS-TCS, which possesses 50 wt % of TCS moieties, was collected (see Supporting Information), and even for this sample, the aromatic C−H stretching peak was quite weak. Because of the weakness of the IR signal, SFG signal of the aromatic C−H stretching modes in TCS cannot be very strong, and was not observed after it was incorporated into the PDMS.

An SFG spectrum of HMS-TCS was collected using a near total reflection geometry using a CaF_2 prism.[59] The SFG signal collected from this geometry should be much stronger. Even so, only a very weak SFG signal for the aromatic C−H stretches of TCS at 3065 cm^{-1} was detected in the ssp or ppp spectra (see Supporting Information). The intensity of the 3065 cm^{-1} peak is only about 1% of the 2910 cm^{-1} peak. From the above FTIR and SFG studies of HMS-TCS, it was concluded that the aromatic C−H signals from TCS moieties are too weak to detect even if significant TCS moiety segregation to the coating surface occurred.

The SFG spectrum collected from sample A0 (pure PDMS) in Figure 4 is dominated by the 2965 cm^{-1} peak, similar to previously published results.[36] This shows that surface dominating $SiCH_3$ groups adopt a different orientation in water than in air. The SFG spectrum collected from sample A1 is not very different than that from A0, indicating that the surface in water is still similar after introducing a small concentration of TCS moieties into the sample. However, for samples 3 to 5, almost no signals can be detected. It is believed that this result is due to the segregation of TCS moieties to the coating surface.

3.1.3. Recovery after Exposure to Water. SFG spectra were collected after contact with water for a short time and then exposure to air (Figure 5). The SFG spectra from all the samples have similar spectral features. The intensities for samples A3, A4, and A5 are weaker than samples A0, A1, and A2. It is hypothesized that samples A0, A1, and A2 were still dominated by PDMS, but for samples A3, A4, and A5, TCS moiety segregation to the surface occurred. Because of this segregation to the surface, the surface coverage of PDMS for samples A3, A4, and A5 was smaller and the PDMS signals therefore decreased substantially. Since the TCS moieties are more hydrophilic than PDMS, the TCS moieties segregate to the surface in water. However, segregation to the surface can only be detected (from the decrease in the PDMS signal) for coatings possessing a relatively high level of TCS moieties. Quantitatively, this study shows that when adding more than 17.5% HMS−TCS or 8.75% TCS surface segregation of TCS moieties can be inferred. The study was also repeated using artificial sea water with similar results.

3.1.4. Interactions between Polymer Surfaces and Fibrinogen. The first step in marine biofouling is the interactions between the coating surface and biomolecules such as adhesive proteins generated by marine organisms. Fibrinogen was used as a model protein to test the coating surface−biomolecule interactions. Even though fibrinogen is not a protein from marine organisms, it is believed that investigations on fibrinogen interactions with polymer surfaces may confirm that coatings with varied amounts of TCS interact with biomolecules differently.

The native structure of fibrinogen has been described as trinodular, with three hydrophobic domains connected by α-helical coiled coils (Figure 6a).[66–70] The elongated 45 nm structures consist of two outer D domains, each connected by a coiled−coiled segment to a central E domain. The E domain contains a nexus of chains that bond the two almost identical halves of a molecule together in a small globular region. Previous

(63) Stafslien, S.; Daniels, J.; Mayo, B.; Christianson, D.; Chisholm, B.; Ekin, A.; Webster, D.; Swain, G. *Biofouling* **2007**, *23*, 45–54.
(64) Stafslien, S. J.; Daniels, J.; Bahr, J. A.; Mayo, B.; Chisholm, B. J.; Pieper, R. J.; Webster, D. C.; Ribeiro, E. *Polym. Prepr. (Am. Chem. Soc., Div. Polym. Chem.)* **2007**, *48*, 149–150.
(65) Casse, F.; Stafslien, S. J.; Bahr, J. A.; Daniels, J.; Finlay, J. A.; Callow, J. A.; Callow, M. E. *Biofouling* **2007**, *23*, 121–130.
(66) Jung, S.; Lim, S.; Albertorio, F.; Kim, G.; Gurau, M. C.; Yang, R. D.; Holden, M. A.; Cremer, P. S. *J. Am. Chem. Soc.* **2003**, *125*, 12782–12786.
(67) Peppas, N. A.; Langer, R. *Science* **1994**, *263*, 1715–1720.
(68) Hubbell, J. A. *Biotechnology* **1995**, *13*, 565–576.
(69) Anderson, J. M. *Annu. Rev. Mater. Res.* **2001**, *31*, 81–110.
(70) Babensee, J. E.; Anderson, J. M.; McIntire, L. V.; Mikos, A. G. *Adv. Drug Delivery Rev.* **1998**, *33*, 111–139.
(71) Clarke, M. L.; Wang, J.; Chen, Z. *J. Phys. Chem. B* **2005**, *109*, 22027–22035.
(72) Wang, J.; Chen, X. Y.; Clarke, M. L.; Chen, Z. *J. Phys. Chem. B* **2006**, *110*, 5017–5024.

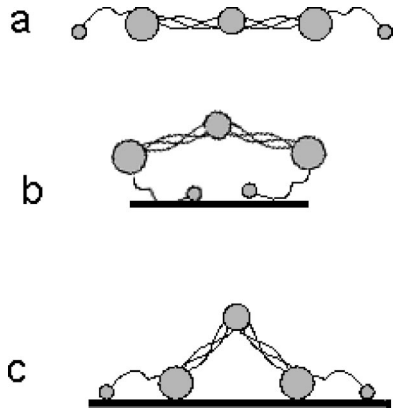

Figure 6. Schematics of native fibrinogen (a) and fibrinogen adsorbed on A4 (b) and A0 (c).

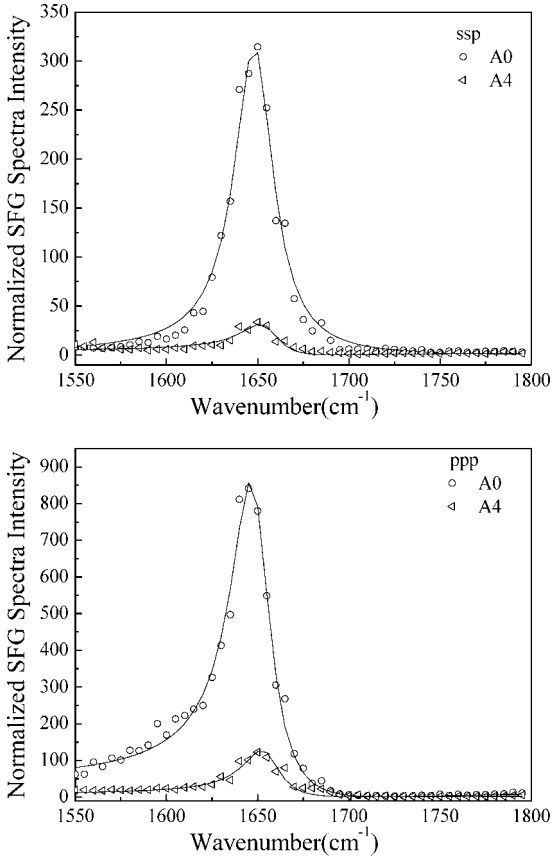

Figure 7. SFG (ssp and ppp) amide I spectra collected from the interfaces between fibrinogen solution and A0 as well as A4.

SFG research has shown that fibrinogen molecules adopted varied structures while adsorbed on various polymer surfaces and have different time-dependent structural changes.[71,72]

Samples A0 and A4 were used in this research. Both ssp and ppp SFG spectra of fibrinogen adsorbed at the interfaces between these two coatings and 1.0 mg/mL fibrinogen solution have been collected and are shown in Figure 7. Figure 7 shows that the signal intensities from fibrinogen adsorbed on sample A0 in both ssp and ppp spectra are much stronger. SFG signal intensity is determined by the surface coverage as well as the orientation of a functional group. FTIR was used to determine the adsorption amount of fibrinogen on samples A0 and A4. Samples A0 and A4 were contacted to 1.0 mg/mL fibrinogen solution for 1 h, and then were washed using deionized water three times. FTIR spectra were collected from these samples and it was determined that

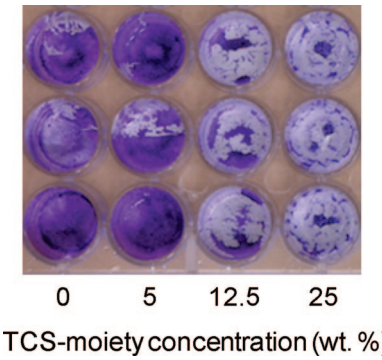

Figure 8. Image of *C. lytica* biofilm surface coverage, after crystal violet staining, on PDMS coatings containing TCS moieties.

the adsorption amount of fibrinogen on sample A0 was about twice that on sample A4. It is believed that, in addition to a larger amount, on sample A0 the fibrinogen adopted a more bent structure, while on sample A4 fibrinogen adopted a more linear conformation. Schematics of the proposed conformations are shown in Figure 6b,c. The fit spectra are shown in Figure 7. The fitting results (the ppp/ssp ratio) also support this conclusion.[71–73]

3.1.5. Evaluation of Antifouling Activity. High-throughput assays based on microorganisms such as bacteria and algae have been used extensively for screening of antifouling performance of experimental coatings. The assays, which have been described in detail by Stafslien and co-workers,[18,62,63,65] involve a preconditioning step by immersion of coating arrays in water to remove any leachable components from the coatings that may be toxic to the microorganisms. To ensure that toxic, leachable components have been removed from the coatings, a leachate toxicity assay is conducted using the microorganisms of interest. Once the coating leachates have been shown to be nontoxic to the microorganism of interest, a biofilm growth and retention assay was conducted to characterize the antifouling performance of the coatings. Using this process, a reduction in biofilm growth and retention can be attributed to the coating surface as opposed to leaching of toxic components. In this study, the marine bacterium *C. lytica* was used to characterize the antifouling properties of PDMS coatings containing TCS moieties. None of these coatings showed any detectable leachate toxicity after 14 days of water immersion (data not shown). As shown in Figure 8, the SFG results correlate well with the antifouling activity of these coatings. The coatings containing TCS moiety concentrations of 0 and 5 wt% (samples 0 and 1) were completely covered by the bacterial biofilm. However, for the coatings containing 12.5 and 25 wt % TCS moieties (samples 3 and 5), the biofilm surface coverage was greatly reduced (80−85%). Examination of the crystal violet extraction data also showed a moderate reduction in biofilm growth and retention (i.e., total biomass) for these two coatings (30−40%). These results suggest that the TCS moieties on the PDMS surface induce a high degree of biofilm retraction[18] (i.e., biofilm redistribution on the coating surface as the surface dries), attributed to poor biofilm adhesion, rather than substantially reduce biofilm growth. This can be seen when examining the plate images in Figure 8. A significant reduction in biofilm growth typically results in a lower intensity of the crystal violet stain over the entire surface of the coating. In this case, the retained biofilm has "retracted" into small, dense areas as a consequence of removal and redistribution of the biofilm during the water evaporation process on the hydrophobic silicone surface. As a result, the retracted areas of dense biofilm stain

(73) Wang, J.; Lee, S. H.; Chen, Z. *J. Phys. Chem. B* **2008**, *112*, 2281–2290.

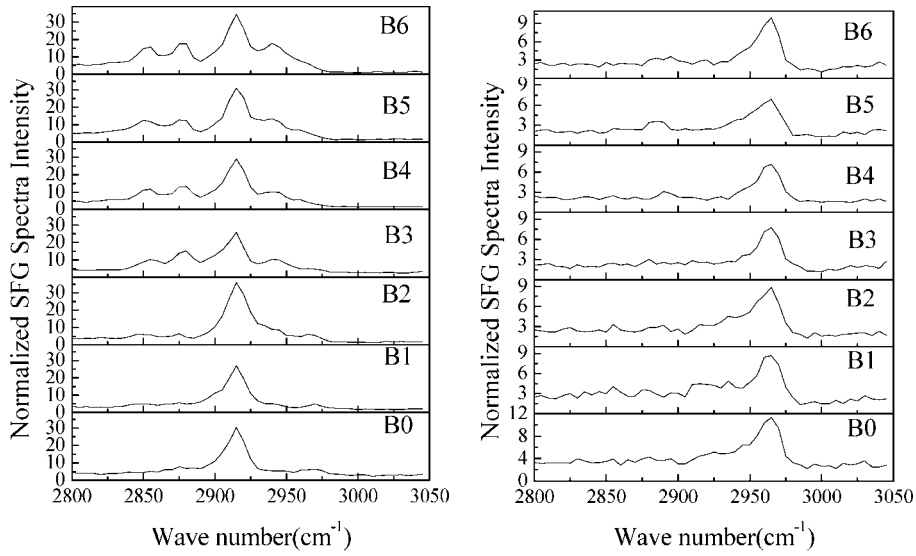

Figure 9. SFG spectra collected from PDMS samples with different amounts of C-14 QAS incorporated in air. (left: ssp; right: ppp).

intensely with the crystal violet dye.

The results of the antifouling activity experiments show that the critical concentration of TCS moieties needed to obtain a significant antifouling effect was between 5 and 12.5 wt %, matching the SFG studies quantitatively. In this regard, SFG results indicated that the critical concentration of TCS segregation to the surface was between 8.75 and 12.5 wt %. This shows that the presence of TCS on the surface results in an antifouling effect.

Overall, the results of this study suggest that SFG can provide a molecular-level interpretation of the antimicrobial activity of these coating systems. However, due to the weak SFG signal generated from TCS moieties, the surface segregation of TCS moieties could not be directly detected. As a result, subsequent studies on PDMS-based coatings containing tethered biocides were focused on biocide moieties derived from quaternary ammonium salts (QASs).

3.2. Surface Structures of PDMS-Based Coatings Containing Tethered C-14 QAS Groups. *3.2.1. Surface Structures of PDMS Incorporated with C-14 QAS in Air.* Similar to the experiments in the previous section, SFG spectra were collected first from surfaces of all seven samples (samples B0 to B6 listed in Table 2) of PDMS incorporated with C-14 QAS in air using the ssp and ppp polarization combinations. As shown in Figure 9, the ppp SFG spectra for all the samples are similar, dominated by the C−H asymmetric stretches of the methyl group at 2965 cm^{-1}, while the ssp spectra of various samples are quite different. The ssp spectrum collected from sample B0, which has no C-14 QAS incorporated, has two peaks at 2915 and 2965 cm^{-1} contributed by the C−H symmetric and asymmetric stretches of the Si-CH_3 group. This is similar to those observed from PDMS surfaces in the previous research. For samples B1−B6, C-14 QAS groups were detected in the ssp polarization combination. In addition to the signals contributed by PDMS Si-CH_3 group stretches, three new peaks at 2857, 2880, and 2940 cm^{-1} were detected on the surfaces of samples B1 and B2 in air. These three peaks become very strong in the ssp spectra collected from samples B3 to B6. These three vibrational peaks were assigned to the CH_2 symmetric stretching, CH_3 symmetric stretching, and CH_3 Fermi resonance modes.[74] It was believed that the signals at 2857, 2880, and 2940 cm^{-1} were contributed by surface-segregated C-14 QAS biocide groups. When a relatively low concentration of C-14 QAS groups was incorporated into PDMS (e.g., samples B1 and B2), its surface segregation was able to be detected. When more C-14 QAS groups were incorporated, more surface segregation (evidenced by stronger SFG signals) was observed (e.g., samples B3 to B6). Peak assignments were confirmed by collecting FTIR transmission spectra from samples B0 to B6. The FTIR spectra collected showed that peaks at 2857, 2880, and 2940 cm^{-1} increased linearly with C-14 QAS group concentration (see Supporting Information).

The ssp spectra displayed in Figure 9 clearly indicate that C-14 QAS groups segregate to the surface and surface coverage generally increases with bulk C-14 QAS concentration. The dominate signal in the SFG spectra collected using the ppp polarization combination is at 2965 cm^{-1}, which is due to the methyl asymmetric stretch. The methyl asymmetric stretching frequencies in the $SiCH_3$ group and the regular CCH_3 group are similar. Therefore, the ppp signal collected from B0 is contributed from the $SiCH_3$ group, but ppp signals from other samples may contain contributions from both $SiCH_3$ groups and regular methyl groups from the C-14 QAS moieties.

To obtain some quantitative information, ssp spectra were fit using eq 2 with 6 peaks at 2845, 2857, 2880, 2915, 2940, and 2965 cm^{-1}. The 2880 and 2940 cm^{-1} peaks were attributed to the methyl symmetric stretching and Fermi resonance modes of the CCH_3 groups from C-14 QAS. The 2845 and 2857 cm^{-1} peaks were from the symmetric stretch of different C-14 QAS methylene groups. The 2915 cm^{-1} peak was attributed to the symmetric stretch of $SiCH_3$ from PDMS. The following ratio was used to characterize the relative surface segregation of C-14 QAS and PDMS:

$$\text{Ratio} = \frac{(A_{2880}/\Gamma_{2880} + A_{2940}/\Gamma_{2940})/2}{A_{2915}/\Gamma_{2915}} \quad (3)$$

where A is the signal strength and Γ is the peak width. This ratio for different samples is plotted in Figure 10 as a function of the weight ratio of C-14 QAS to PDMS. As shown in Figure 10, when a small amount of C-14 QAS was incorporated, e.g., in samples B1 and B2, a weak signal of C-14 QAS comparing to that of PDMS was detected. When more C-14 QAS was incorporated, e.g., in samples B3 to B6, stronger SFG signal of

(74) Gragso, D. E.; McCarty, B. M.; Richmond, G. L. *J. Am. Chem. Soc.* **1997**, *119*, 6144–6152.

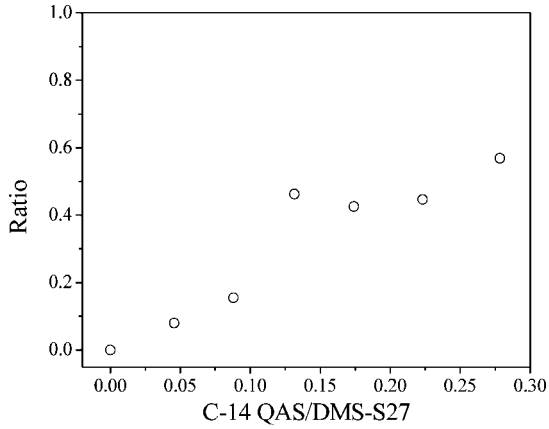

Figure 10. The ratio defined in eq 3 was plotted against the weight ratio of C-14 QAS versus DMS-S27.

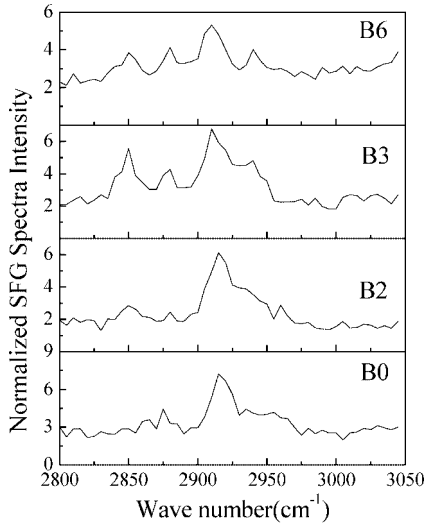

Figure 11. SFG spectra collected from PDMS samples with different amounts of C-14 QAS incorporated in water.

C-14 QAS was observed. A large change in the ratio occurred between B2 and B3.

3.2.2. Surface Structures of PDMS Incorporated with C-14 QAS in Water. Since the application for these PDMS materials is for an aqueous environment, SFG spectra were collected from the surfaces contacted to water (Figure 11). The spectra for samples B1 and B2 are similar and the spectra for samples B3 to B6 are similar. For the SFG spectra collected from B0, B2, B3, and B6 surfaces, the SFG signal intensities in water are much weaker than those in air. Part of the weakness (about a factor of 3) is due to the difference in Fresnel coefficient,[27,28,53] or possibly more disordered surfaces in water. PDMS SFG (ssp) signal (2915 cm^{-1}) was detected from the surfaces of all samples. Discernable SFG signals from biocide were observed from the surfaces in contact with water of samples B2 and B6.

SFG spectra were also collected from these samples after being in contact with water for a short time and exposure to air. The spectra (not shown) are similar to those observed in air before having contact with water. Both PDMS and C-14 QAS were observed simultaneously on the surfaces of samples B1 to B6.

3.2.3. Evaluation of Antifouling Activity. Figure 12 displays antifouling results for PDMS coatings containing QAS moieties obtained using *C. lytica* and *N. incerta*. The results show that the coatings were ineffective at reducing the biofilm growth of *C. lytica*. In contrast, the coatings showed increasing antifouling

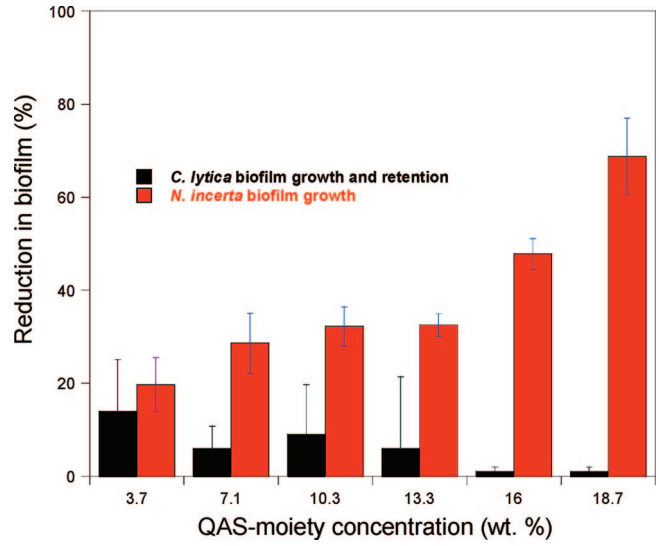

Figure 12. Antifouling performance of PDMS coatings containing QAS moieties toward *C. lytica* and *N. incerta*.

Table 3. Antimicrobial Activity of PDMS with C-14 QAS

sample no.	percent reduction in biofilm growth	standard deviation for the percent reduction in biofilm growth
B1	19.7	5.8
B2	28.6	6.5
B3	32.2	4.2
B4	32.5	2.4
B5	47.8	3.3
B6	68.8	8.2

performance toward *N. incerta* with increasing QAS content. Variations in antifouling performance with respect to microorganism species are not unexpected since the cell wall composition and structure are drastically different between the two organisms. The microfouling algae, *Navicula*, has a cell wall structure composed of silica, while the Gram-negative marine bacterium, *C. lytica*, has an outer cell membrane composed of lipopolysaccharides and proteins. As a result, the C-14 QAS on the PDMS surface may interact differently with the cell wall structures and account for the difference observed in antifouling activity with respect to these two marine organisms. Even though the antifouling results obtained with *N. incerta* cannot be quantitatively related to the SFG results shown in Figure 10, the similar general trend can be observed: the more C-14 QAS incorporated, the stronger SFG signal from QAS, the greater the reduction in algal growth.

SFG signal intensities are determined by both surface coverage and surface orientation of functional groups. It is possible that, when different amounts of C-14 QAS were incorporated into PDMS, the surface orientation of C-14 QAS varied. Therefore, the signal intensity can only be qualitatively but not quantitatively related to the surface coverage of C14-QAS. The results in Figure 10 cannot be correlated to the algal assay data (Table 3) quantitatively. However, as mentioned above, SFG results do show that generally the higher the C-14 QAS intensity, the more reduction in algal growth.

Conclusion

The molecular-level surface structures of PDMS coatings containing different amounts of the biocides Triclosan (TCS) and tetradecyldimethyl (3-trimethoxysilylpropyl) ammonium chloride (C-14 QAS) in air, in water, and after removing from

water and exposing to air again were studied using sum frequency generation (SFG) vibrational spectroscopy. The SFG spectra collected from the surface of PDMS incorporated with TCS in air were dominated by the C−H symmetric and asymmetric stretches of the Si-CH_3 groups. SFG spectra collected in water imply that TCS moieties may segregate to the polymer surface. After contact with water, the SFG intensity showed decreases between the TCS contents of 8.75% and 12.5%. The decrease in SFG intensity could be because TCS segregates to the surface where TCS generates extremely weak SFG signal. An excellent correlation has been found between our SFG results and the results of the antifouling activity experiments. In addition, molecular interactions between a model protein, fibrinogen, and PDMS with or without TCS incorporated were examined. Results demonstrate that fibrinogen adopts different conformation/orientation, due to different interactions induced by the presence/absence of TCS on the surface.

Surface segregation and surface coverage of biocides were directly detected on PDMS with C-14 QAS incorporated in air and in water. The PDMS surface-dominating Si-CH_3 groups, biocide SFG signal from CH_2 symmetric stretch, CH_3 symmetric stretch, and CH_3 Fermi resonance modes were detected on the surface of the samples incorporated with C-14 QAS. Qualitatively, the SFG results can be related to antifouling activity.

It was concluded in general that only after incorporating a certain amount of biocide into the PDMS matrix can enough of biocide segregate to the surface to exhibit an antifouling effect. It has been debated whether surface modification can improve the antifouling performance of polymer coatings, because it has been speculated by some that the initial preconditioning film or the establishment of a microbial biofilm will eventually cover the polymer coating surface, enabling biofouling to occur. Our research shows that biocides can segregate to the PDMS surface to change the surface structure, which influences biofilm formation. This surface restructuring was shown to enhance the antibiofouling property of the polymer coating.

In the future, molecular interactions between PDMS incorporated with biocides and adhesive proteins generated from marine organisms such as mussel proteins and barnacle proteins, or marine organisms themselves, such as Ulva spores, will be examined using SFG to elucidate more details about how biocides mediate antifouling activity.

Acknowledgment. This work is supported by the Office of Naval Research (N00014-02-1-0832, N00014-06-1-0952, and N00014-07-1099). We thank David Christianson for his help in this research.

Supporting Information Available: FTIR spectra of PDMS incorporated with biocides. SFG spectra collected from HMS-TCS. This material is available free of charge via the Internet at http://pubs.acs.org.

LA800769Z